IOP Publishing Superconductor Science and Technology
Supercond. Sci. Technol. **38** (2025) 085007 (13pp) https://doi.org/10.1088/1361-6668/adedbd

Demonstration of current sharing around tape defects in a low-inductance CORC® wire solenoid generating a peak magnetic field of 4.6 T at 25 K

Jeremy D Weiss[1,*], Danko van der Laan[1,2], Chul H Kim[3,4], Reed Teyber[5], Kyle Radcliff[2], Virginia Phifer[5], Daniel S Davis[5], Yifei Zhang[7], Lance D Cooley[5] and Sastry V Pamidi[3,4]

[1] University of Colorado, Boulder, CO 80309, United States of America
[2] Advanced Conductor Technologies LLC, Boulder, CO 80301, United States of America
[3] Center for Advanced Power Systems, Florida State University, Tallahassee, FL 32310, United States of America
[4] FAMU-FSU College of Engineering, Tallahassee, FL 32310, United States of America
[5] National High Magnetic Field Laboratory, Tallahassee, FL 32310, United States of America
[6] Lawrence Berkeley National Laboratory, Berkeley, CA 94720, United States of America
[7] SuperPower Inc., Glenville, NY 12302, United States of America

E-mail: Jeremydavidweiss@gmail.com

Received 11 April 2025, revised 19 June 2025
Accepted for publication 9 July 2025
Published 7 August 2025

Abstract

This manuscript presents the design, fabrication, and operation of high temperature superconducting conductor on round core (CORC®) wires utilizing variable critical current REBCO tapes that contain occasional dropouts of critical current (I_c). Performance evaluations conducted at temperatures ranging from 25 K to 77 K demonstrated comparable superconducting characteristics between CORC® wires with and without intrinsic variations in I_c within the REBCO tapes. This is a clear indication that the high level of current sharing between tapes in CORC® wires allows current to bypass local defects. A 70 mm bore, 4-layer CORC® solenoid in which 25 m of CORC® wire was wound into 81.5 turns, generated a peak magnetic field of 4.6 T at an I_c of 4460 A at 25 K. The I_c of the solenoid corresponds closely with the sum of the expected average tape I_c, not its minimum I_c driven by the tape dropouts. Experimental results confirmed stable dissipative operation at 4021 A (87% I_c) continuous current with minimal power losses, highlighting the feasibility of manufacturing longer-length CORC® conductors from tapes with significant local dropouts for superconductor applications including fusion, accelerators, power transmission, and rotating machinery.

Keywords: CORC, HTS magnet, defect tolerant

* Author to whom any correspondence should be addressed.

1. Introduction

High temperature superconductors (HTS) are an enabling technology to generate high magnetic fields at temperatures above 20 K, enabling the construction of efficient superconducting machines like motors, generators, and fusion confinement devices that would otherwise be difficult to economically produce using low temperature superconductors (LTS) due to the costs and difficulty of managing heat loads at lower temperatures. REBCO coated conductors along with Bi 2212 and Bi2223 have emerged as some of the most promising HTS materials for applications [1–3]. However, manufacturing long-length REBCO conductors with consistent properties continues to be a challenge due to limited batch lengths and sporadic dropouts of current carrying performance that reduce yield and require sectioning of the produced conductor into shorter lengths to remove the dropouts.

Several approaches to mitigate the impacts of localized variations in critical current (I_c) have focused on magnet designs with improved defect-tolerance, such as no-insulation or partially insulated pancake coil designs for REBCO tapes that take advantage of current-sharing between individual strands of conductor to avoid normal zones that might otherwise result in a thermal runaway condition [4–7]. These approaches rely on low turn-to-turn resistance that helps protect the magnet by providing additional thermal stability through enabling additional electrical paths for current. A similar approach has been adopted for high current cables consisting of several REBCO tapes, where current sharing between soldered strands within the cable has proven to provide similar benefits [8–11]. Here, we explore whether current sharing between tapes in CORC® wires is sufficient for current to bypass local defects without the need to solder the conductor. This would have the added advantage of keeping the tapes unbonded, which maintains the conductor's bending flexibility and high tolerance to axial tensile strain [12, 13]. Instead, the CORC® cable topology relies on sliding pressure contacts between tapes to allow for adequate current sharing within the conductor [8, 10, 11].

The contact pressure between tapes within CORC® cables has previously been calculated[14],while experiments have been carried out to quantify tape-to-tape contact resistivity as a function of pressure [10, 11]. While extensive models have been developed to evaluate variations of tape-to-terminal [15, 16] or cable-to-terminal [15, 17] properties of CORC® cables, real models considering tape-to-tape contact resistance for long-length cables containing dropouts are lacking. Recent work on models for short cables, including a network model [8] have only just began to shed light on the advantages and possible new capabilities of CORC® cables with high level of current sharing resulting from the helical wind of the tapes under maintained tension.

The motivation of this work is to provide evidence that robust long-length high-current REBCO conductors can be manufactured and wound into magnets and operated at temperatures rangeing from 20–77 K using either liquid bath or conduction cooling. By relying on current perculation within high tape-count cables at manageable dissipation, we provide a route to produce cables that not only reduce costs by loosening the specifications of run-of-the-mill conductors, but also provides evidence that the inclusion of tape-to-tape joints would allow the production of CORC® cables and wires at km length-scales while tape lengths available are still limited to less than a km. These two traits open up new possibilities especially for rotating machines, fusion, and power transmission where longer conductor lengths are desired.

2. Experimental methods

2.1. Measurement procedure

CORC® wires were wound at Advanced Conductor Technologies from 2 mm wide SuperPower tapes. The tapes consisted of a REBCO film deposited on 30 μm thick Hastelloy substrate and then surround deposited with 1–3 μm of silver and approximately 5 μm of copper. The REBCO tape critical current performance was evaluated using a Reel-to-Reel Tapestar™ system at SuperPower Inc. Tapes delivered by SuperPower included pristine tapes without any significant defects and so-called variable I_c (VIC) tapes that contain one, or more steep local dropouts. Transport measurements of voltage (V) as a function of current (I) use a fit of electric field versus current to determine I_c and N using the following equation:

$$E = I\left(\frac{R}{L}\right) + E_c\left(\frac{I}{I_c}\right)^N - E_0$$

where E is the electric field (measured voltage divided by L, the length of conductor within a given region of peak field), E_c is the electric field criterion of 1 μV cm^{-1}, R is the linear resistance, and E_0 is an electric field offset. N is a fitting parameter that quantifies the sharpness of the superconducting to resistive transition. L was chosen as 20 cm for the tapes, 9.6 m for the short CORC® coils, and 4.4 m for the 81.5-turn CORC® solenoid wound from VIC tapes, which is the length of the CORC® wire in the innermost turn over which the superconducting to resistive transition likely occurs.

Transport I_c as a function of applied magnetic field (B) measurements on single tapes were performed in subcooled liquid nitrogen using a closed cryostat and a copper electromagnet to vary the field from 0 to 1.5 T. High current measurements on a short CORC® wire were carried out from 65–76 K in a liquid nitrogen bath using an anti-cryostat within a cryomagnetics split-pair 8 T superconducting magnet. Temperature was controlled by varying the pressure of the nitrogen bath using a calibrated Lakeshore Cernox sensor located in the high field zone next to the sample where a calibrated Lakeshore Hall sensor was used to measure the central field. Figure 1 shows a schematic of the measurement setup.

Single layer coils were made using CORC® wires wound from pristine (baseline) or VIC tapes by wrapping the wire

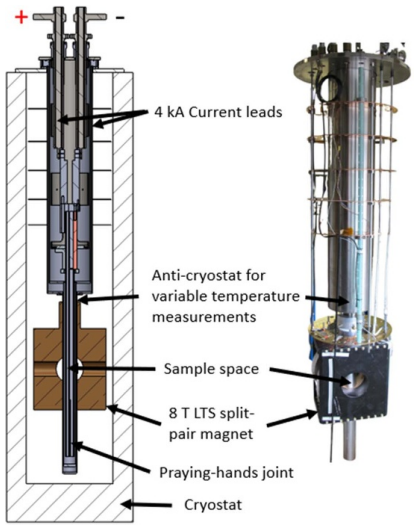

Figure 1. Overview (left) and picture (right) of the insert and split pair LTS magnet that allows measuring of I_c of straight samples at fields up to 8 T in liquid nitrogen between 65 and 77 K.

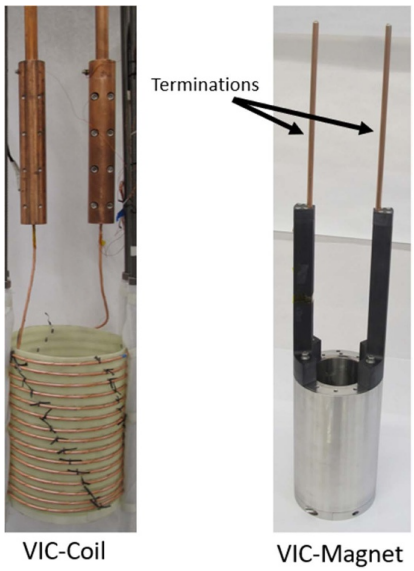

Figure 2. Pictures of loosely wound 15 turn VIC-Coil (left) and 81.5 turn, 4-layer CORC® VIC-Magnet (right).

around a 178 mm OD garrolite tube with 1.27 cm between turns (see figure 2). This spreading out of the turns was done to keep the field of the windings low, with a calculated transfer function for a 15 turn coil of 82 mT kA^{-1} on the conductor. Voltage tap wires were embedded within the terminations between the copper tube and the CORC® wire approximately 2–3 cm from where the cable exits the terminations. The voltage tap wire was then co-wound around the conductor to produce a return path for voltage signals measured over the coil. This minimizes signal noise by compensating for the inductive pickup of the coil [16]. $V(I)$ performance was measured in boiling liquid nitrogen in a closed cryostat at 65 K and 76 K.

The CORC® solenoid wound from VIC tapes shown in figure 2 was tested within a custom high-current variable temperature measurement system (see figure 3(a)). The system consists of a two-stage stirling cryogenics cryocooler with a forced flow 20 Bar helium gas circulation loop that is routed into a vacuum insulated cryostat to allow sample cooling down to 20 K. Current is supplied through liquid nitrogen (LN_2) cooled busbars that are connected to flexible CORC® current feeders rated for 10 kA of continuous current. The feeders consist of four He gas lines (two inlet and two outlets) and four CORC® cables (see figure 3(b)). The system takes about 5 h to cool the cold mass from room temperature down to below 30 K. The coil is located in a vacuum space and cooled via conduction through copper plates clamped onto the coil through which the helium gas is circulated.

2.2. Design of CORC® wires

Figure 4 shows I_c as a function of magnetic field applied perpendicular to the tape surface at 65 K for various short samples of 2 mm wide tapes (named S1–S10) compared to reference data taken from a database[18]. To ensure the design of a reasonably compact magnet operating at an engineering critical current density (J_e) exceeding 100 Amm^{-2} at 65 K and 1.5 T, we chose a standard CORC® wire layout for a 3.6 mm diameter conductor containing between 27 and 30 2 mm wide tapes. Such wires should result in an I_c (65 K, 1.5 T) of at least 1050 A, but depending on the tapes used, could be twice as high.

Tapes were characterized at 77 K in self-field using a reel-to-reel Tapestar™ magnetization measurement system to determine I_c as a function of position. Tape sections with minimal I_c variations were used to manufacture two baseline CORC® wires, one straight section measuring 1 m (Baseline-Short), and one single layer coil wound from a 10 m long CORC® wire (Baseline-Coil). VIC tapes containing 1 or more defects (defined as an I_c drop exceeding 15% of the tape's average I_c) were used to make two VIC CORC® wires: one 10 m section wound into a single layer coil (VIC-Coil), and one 25 m section wound into a compact solenoid with a 70 mm diameter clear bore (VIC-Magnet). For the VIC wires, the severity of I_c dropouts varied for each piece of tape. No optimization was carried out to preferentially space out the dropouts, but the summation of the minimum tape I_c (Σtape I_c^{min}) aimed to be approximately 50% of the summation of the average tape I_c (Σtape I_c^{ave}). For instance, the 10 m long VIC-Coil and 25 m long VIC-Magnet had an average I_c^{min}/I_c^{ave} of 51% (STD 27%) and 48% (STD 26%), respectively. Figure 5 shows the I_c derived from the Tapestar™ scans overlayed as a function of CORC® wire index for each of the samples. For clarity, individual plots of each layer's Tapestar™ scan can be found in the appendix. The properties

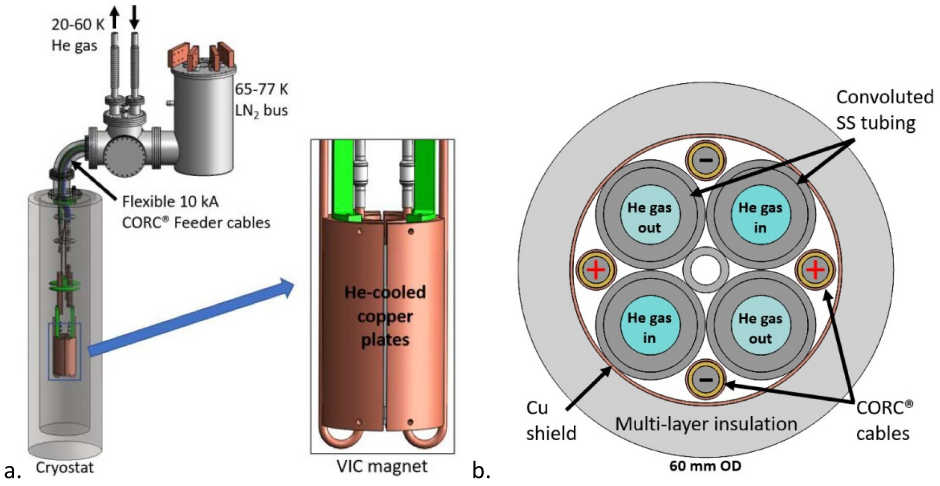

Figure 3. (a) High-current variable temperature test platform used for CORC® magnet characterization. (b) Schematic of a cross-section of the flexible 10 kA feeders containing four 5.8 mm CORC® cables and four high pressure He gas coolant lines.

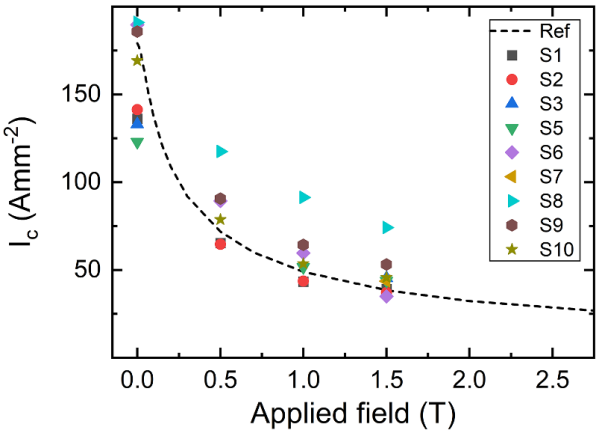

Figure 4. Critical current as a function of applied field for various 2 mm wide tapes measured at 65 K. Dotted line is data from [19] after scaling to 2 mm width.

of the CORC® wire samples manufactured are summarized in table 1.

2.3. Design of the CORC® solenoid

The CORC® VIC-Magnet was dry wound from 25 m of CORC® wire, containing 27 tapes of 2 mm in width (see figure 7). The magnet consisted of 81.5 turns through 4 layers with coil dimensions shown in table 2. Full-hard 316 stainless steel shim foil coiled to 1 mm thickness was used between each layer to reinforce the coil. Glass fiber sheathing was wound in the outer gap between the windings. After winding, the coil was bottom filled with Stycast 2850 epoxy. The VIC-Magnet has a peak transfer function of 1.03 T kA^{-1}. At $I = 4800$ A, the coil would produce a peak field of 5 T as shown in the 2D color contour plot of the calculated magnetic flux density for half of the magnet shown in figure 6.

The isotropic bending flexibility of the CORC® wire allowed the conductor to make a compound bend out of the coil-pack and into an s-bend through G10 slots between the coil support and the terminations (see figure 7(a)). The purpose of the flexible s-bends follows the approach developed for the CORC® feeders of the NHMFL 32 T user magnet to allow for movement between the coil support and the coil terminations due to misalignment, mismatches in thermal expansion coefficients, and potential movements during coil centering in a background field [19, 20]. The CORC® wires and voltage taps were terminated within solder-filled copper tubes measuring 6.35 mm in diameter and 210 mm in length.

3. Results

The 1 m long CORC® wire Baseline-Short was prepared to determine the in-field performance of a 30-tape CORC® wire

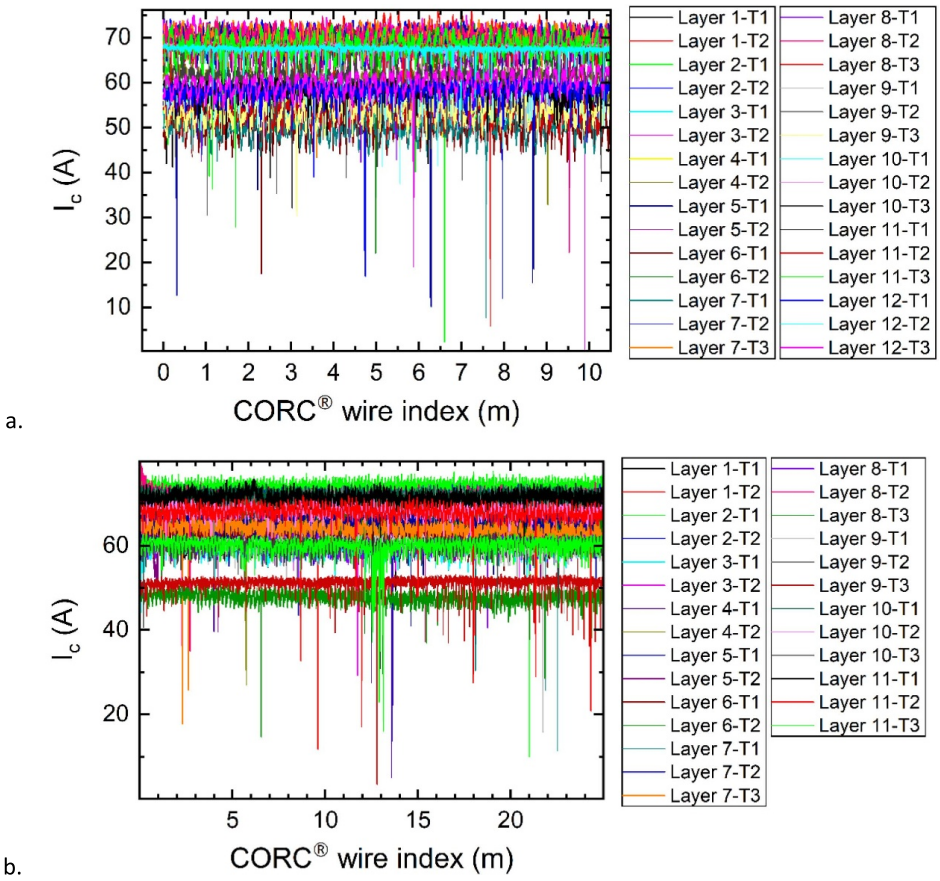

Figure 5. I_c as a function of CORC® wire index for all 2 mm wide tapes within (a) the 10 m long CORC® wire used to manufacture VIC-Coil, and (b) the 25 m long CORC® wire used to manufacture VIC-Magnet. For clarity, individual plots of each layer's Tapestar™ scan can be found in the appendix.

Table 1. Properties of the different CORC® wires studied.

Sample name	Diameter (mm)	# of tapes	Length (m)	Σtape I_c^{ave} (A) [77 K]	Σtape I_c^{min} (A) [77 K]
Baseline-Short	3.70	30	1	1896	1800
Baseline-Coil	3.66	30	10	1679	1651
VIC-Coil	3.76	30	10	1848	919
VIC-Magnet	3.61	27	25	1757	843

Table 2. CORC® magnet winding dimensions.

	ID (mm)	OD (mm)	Height (mm)	Turns/ layer
Layer 1	74.0	81.2	69.4	19.0
Layer 2	83.2	90.5	73.0	20.0
Layer 3	92.5	99.7	76.7	21.0
Layer 4	101.7	109.0	80.3	21.5

wound from pristine tapes in the temperature range of 65–75.5 K. Figures 8(a)–(c) show the superconducting to resistive transition by plotting $E(I)$ at applied fields up to 8 T. Figure 8(d) shows the magnetic field dependence of I_c at 65 K, 70 K, and 75.5 K. I_c, N-value, and J_e are summarized in table 3. The I_c at 65 K and 1.5 T is 1459 A (N-value = 16), and the J_e is 136 Amm^{-2}.

Two 10 m long CORC® wires were tested in liquid nitrogen as loosely wound single layer coils. One was wound from pristine tapes (Baseline-Coil) and the other from VIC tapes (VIC-Coil). While the coils both had 30 tapes, Σtape I_c^{ave} of VIC-Coil was 1848 A while the Baseline-Coil had a slightly lower Σtape I_c^{ave} of 1679 A. However, Σtape I_c^{min} was significantly lower for VIC-Coil, at 919 A. Figures 9(a) and (b) shows the electric field as a function of current for the Baseline and VIC coils at 76 K and 65 K. There is little difference in the general $E(I, T)$ characteristics of the conductors.

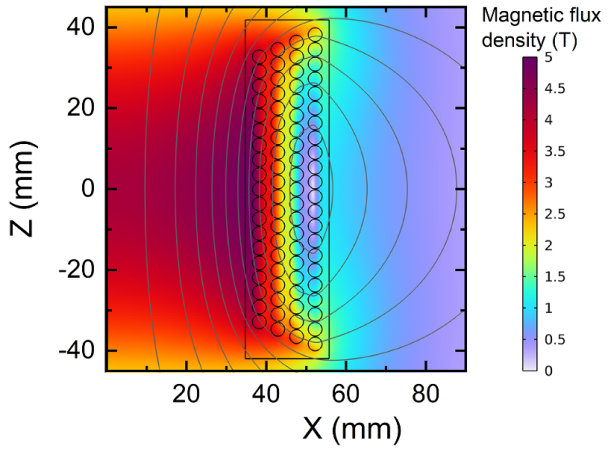

Figure 6. Calculated magnetic flux density from a 2D cross-section of half the coil pack for VIC-Magnet at $I = 4800$ A.

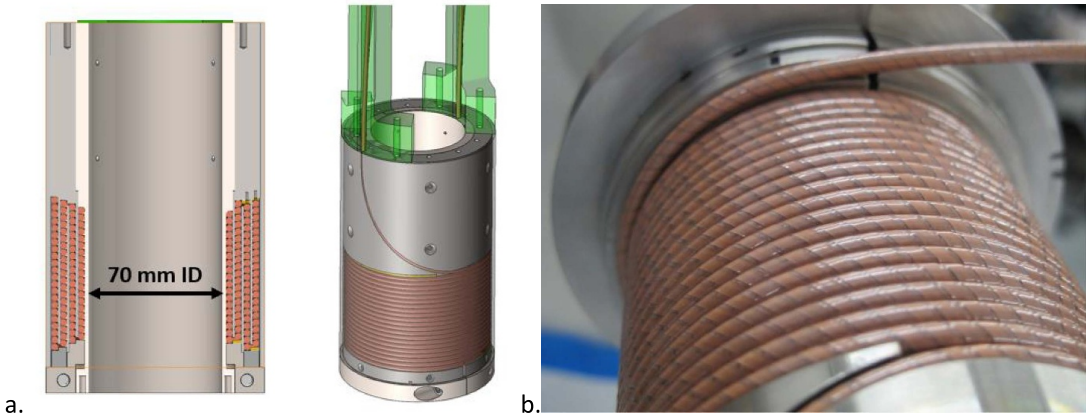

Figure 7. (a) Cross-section and internal view of the 81.5 turn CORC® magnet in its stainless-steel support structure. (b) Picture of VIC-Magnet being wound.

To evaluate the stability of VIC-Coil, current was ramped to 2450 A (89% I_c) at 65 K and held constant for 200 s. Figure 10 shows that the bath temperature and voltage over the coil terminations remained constant following the decay of an inductivly driven voltage during the current ramp. Because the total voltage is measured over the terminations, some of the voltage measured is due to the contact resistance within the terminations. The rest of the voltage then likely comes from the voltage required for current to share around the defects within the cable. The calculated total dissipation is low, at 0.67 W.

The magnet wound from 25 m of 27-tape CORC® wire (VIC-Magnet) was tested at various temperatures in both a liquid nitrogen bath and via conduction using cryogenic helium gas. Figure 11(a) shows the voltage as a function of current after subtracting the inductive voltage offset (V_0). Measurements at 25–60 K were carried out at 49 A s^{-1}, while much slower ramps were used for the measurements at 65 K and 77 K. At 49 A s^{-1}, V_0 was 16.3 mV resulting in an inductance of 0.33 mH. I_c as a function of temperature is shown in figure 11(b) and the data are summarized in table 4. Measurements in the liquid nitrogen bath, where there is significantly more cooling power available, tended to have a more gradual $V(I)$ transition (lower n-value) while measurements in the helium gas cooled setup tended to transition more sharply (higher n-value). For this reason, there is a discrepancy in the I_c (T) dependence shown in figure 11 between the two cooling mediums. There's also the presence of a shoulder in the $V(I)$ transitions of figure 11(a) that's more pronounced at higher current ramp-rates. To evaluate the stability of the magnet at high current with helium gas cooling, the magnet was ramped to 4021 A (87% I_c) at 25 K and current was held constant for

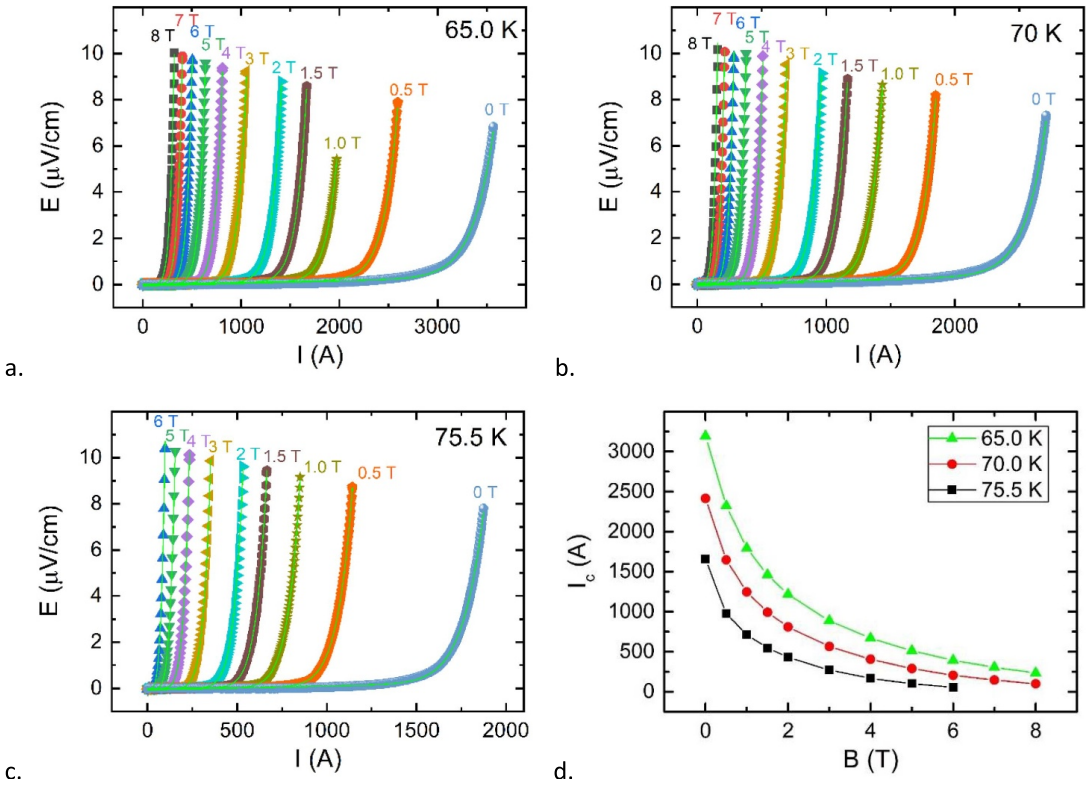

Figure 8. Electric field as a function of current and applied fields for the 1 m long CORC® wire with 30 2 mm tapes (Baseline-Short) measured at (a) 65 K, (b) 70 K and (c) 75.5 K. (d) Critical current plotted as a function of applied field at the different temperatures. Data was taken in liquid nitrogen at a ramp rate of 50 available at: . The green lines in (a), (b), and (c) are the fits used to determine I_c and N-value.

Table 3. Properties at different magnetic fields of 1 m Baseline-Short CORC® wire at 65 K, 70 K, and 75.5 K.

	65 K			70 K			75.5 K		
B (T)	I_c (A)	N-value	J_e (Amm-2)	I_c (A)	N-value	J_e (Amm-2)	I_c (A)	N-value	J_e (Amm-2)
0.0	3195	17	297	2417	17	225	1656	16	154
0.5	2322	18	216	1646	17	153	975	14	91
1.0	1794	17	167	1247	15	116	712	12	66
1.5	1459	16	136	993	14	92	547	11	51
2.0	1216	14	113	811	13	75	431	11	40
3.0	886	13	82	565	11	53	272	9	25
4.0	668	11	62	405	10	38	169	7	16
5.0	512	10	48	290	9	27	101	6	9
6.0	395	9	37	206	7	19	57	4	5
7.0	306	8	28	146	6				
8.0	235	7	22	100	5				

60 s. Figure 12(a) shows the measured current, voltage, and central field during the experiment. As current plateaus, the voltage over the coil decays down to a constant 0.13 mV where dissipation of the coil is only 0.52 W. At 4021 A, the CORC® wire has a J_e of 395 A mm^{-2} and the coil produces 3.5 T at its bore. Figure 12(b) shows the measured axial magnetic field compared to calculated fields up to 4500 A where the conductor experiences a peak field up to 4.6 T.

4. Discussion

The testing of long-length CORC® wires and coils containing variable I_c tapes demonstrate that the performance of the conductor can be nearly identical to that of CORC® wires wound from tapes without dropouts within a dissipative regime. Similar results have been presented for coils consisting of soldered tapes [4] or fusion cables [21, 22] under development,

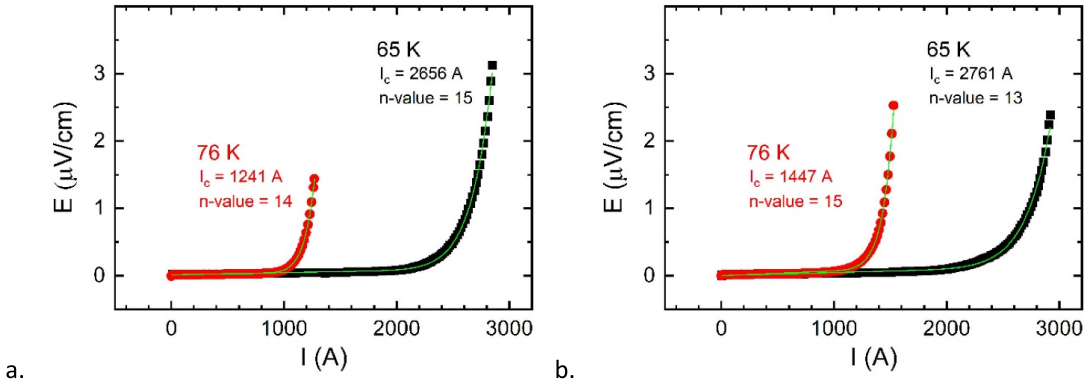

Figure 9. Electric field as a function of current showing the superconducting to resistive transition at 65 K and 76 K for (a) Baseline-Coil and (b) VIC-Coil. Data was taken at a ramp rate of 50 A s^{-1}. The green lines are fits to determine I_c and N-value.

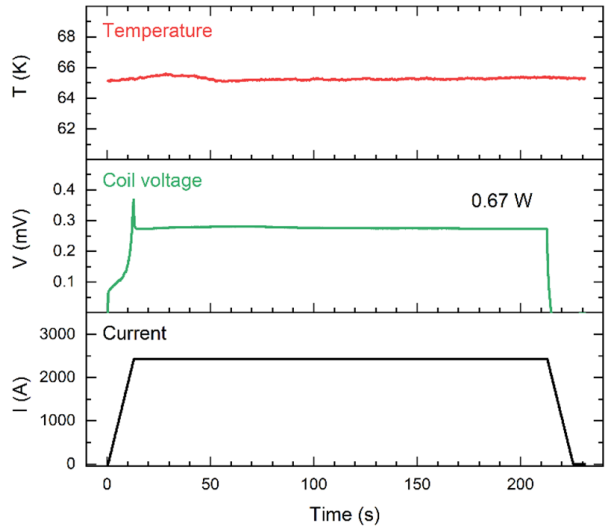

Figure 10. Temperature, electric field, and current as a function of time for the steady-state operation of the 10 m long VIC-Coil. Shown is the dissipation (0.67 W) that is a combination of the terminal resistance and dissipation within the CORC® wire due to current sharing.

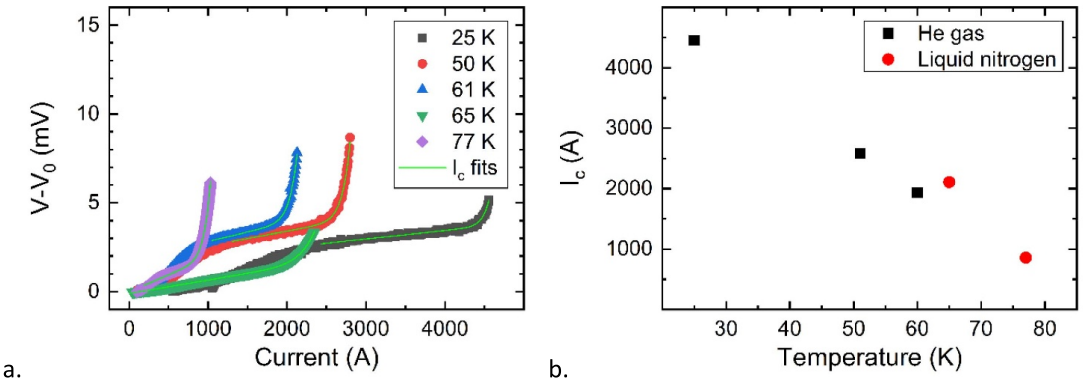

Figure 11. (a) Voltage as a function of ramped current for VIC-Magnet at different temperatures. The green lines are fits to determine I_c and N-value (b) critical current as a function of temperature.

Table 4. Transport properties of VIC-Magnet.

T (K)	Ramp-rate (A s^{-1})	I_c (A)	N-value	R ($\mu\Omega$)	Center field[a] (T)	Peak field[a] (T)
77	29	860	12	1.91	0.76	0.89
65	10	2110	13	0.75	1.86	2.17
60	49	1937	23	1.07	1.70	2.00
51	49	2586	28	0.84	2.28	2.66
25	49	4460	56	0.48	3.92	4.59

[a] At I_c.

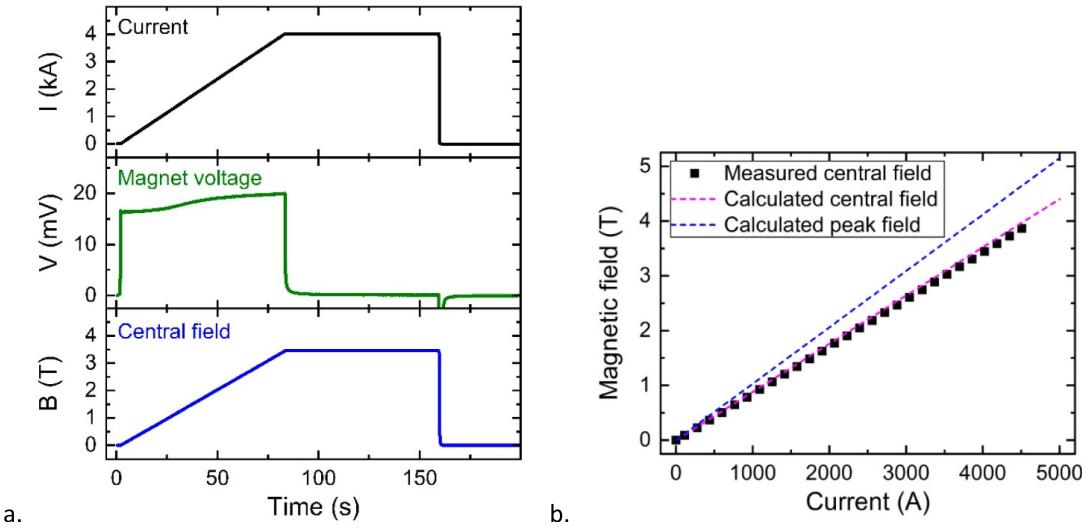

Figure 12. (a) Current, voltage, and measured central field of VIC-Magnet as a function of time at 25 K. (b) Calculated peak and measured central magnetic field as a function of current at 25 K.

where a high level of tolerance to the effect of localized dropouts has been observed especially at elevated temperatures (>20 K) where the heat capacity and thermal stability of the conductor is higher than at 4 K. This depends on the efficacy of current sharing and cooling within a cable or wound coil. A distinct advantage of the CORC® cable topology is that each layer of the cable consists of 2–4 parallel tapes, so a middle tape might have direct electrical contact to 4–8 tapes within neighboring layers. This offers an advantage over a stacked tape approach such as a pancake coil, where each tape is only in direct electrical contact with two neighboring tapes.

Comparing VIC-Coil to Baseline-Coil, we see in table 1 that VIC-Coil by design has about 10% higher Σtape I_c^{ave}, a difference of 169 A. When measured at 77 K and 65 K, the VIC-Coil still outperforms the Baseline-Coil with 17% and 4% higher I_c, respectively. However, it is worth noting that a broader superconducting to resistive transition (lower N-value) is observed for the VIC-Coil in the 65 K data fits. Since the coils are wound in a single layer with equivalent turn-to-turn spacing it is likely that most of the conductors see an equivalent magnetic field distribution.

An approximation for expected CORC® wire performance can be obtained by taking I_c(B, T) data from the University of Vicoria's HTS database [18] in A/mm-width and multiplying by the width and number of tapes within the CORC® wire. Figure 13(a) shows the expected I_c(B) performance at various temperatures compared to VIC-Magnet's load line and measured I_c (B, T). Surprisingly, the performance exceeds the referenced data, except at 25 K where the coil quenches a few hundred amps below the expected current. Figure 13(b) shows a comparison of I_c(B) at 65 K between VIC-Magnet, VIC-Coil, Baseline-Short, and reference data. The single layer VIC-Coil data, that generates about 226 mT at I_c, agrees well with both the Baseline-Short and reference data that were taken in externally applied magnetic fields. This validates that the VIC tapes do not significantly affect the I_c performance of the CORC® conductor in these conditions. However, we measured 74% higher I_c in the VIC-Magnet than even in the Baseline-Short sample at 2 T applied field that contained no VIC tapes. The field map of figure 6 illudes to a relevant fact, that most of the conductor sits at relatively low field compared to the inner layer, and therefore are being operated at a higher margin of their critical current where localized decreases of I_c within the tapes are better tolerated than for the inner layer of the coil. For this reason, a lower L was chosen for the I_c criterion, corresponding to the length of the innermost layer that likely

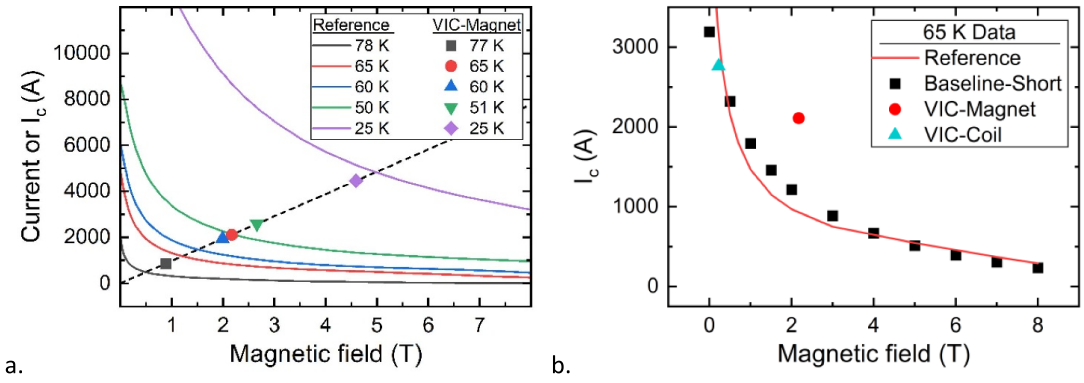

Figure 13. (a) Current (dashed line) or critical current (solid line and symbols) as a function of magnetic field and temperature for a 27 tape CORC® wire. Solid lines are calculated using data from van der Laan *et al* [19] multiplied by 27 × 2, while solid symbols are data reported here for VIC-Magnet. Dashed line is the load-line for the peak field on the CORC® magnet. (b) Critical current vs magnetic field for Baseline-Short, VIC-Magnet, and VIC-Coil compared to van der Laan *et al* [19] multiplied by 30 × 2.

transitions from superconducting to resistive before the rest of the coil. However, figure 6 also shows that the peak field even for the inner layer is primarily oriented on the edge of the conductor where the tape faces are more parallelly aligned with the field, and therefore tape anisotropy may also explain why the I_c performance seems to exceed that of the expected performance of even the Baseline-Short cable that had its entire cross-section exposed to a more uniform magnetic field.

Another point to discuss is the presence of a shoulder in the $V(I)$ curves of figure 11(a). The magnitude of this shoulder appears to be ramp-rate dependent, being much more pronounced for the measurements in He-gas that were carried out at a faster ramp-rate (49 A s^{-1}) than the measurements done in liquid nitrogen (10–29 A s^{-1}). It also only exists in increasing current, disappearing when current is paused (figure 12) or reversed. This suggests the voltage deviation is an inductively or magnetization driven voltage component, and not necessarily due to the presence of VIC tapes in the coil. Similar results were observed on a previously tested CORC® coil, containing no VIC conductor [23].

Steady-state testing (figures 10 and 12), where current is held constant, allows us to evaluate dissipative voltages more accurately over the cables in the absence of inductive voltages caused by current ramping. These tests also allow us to evaluate the thermal stability of the conductors. If dissipation is localized, then heating can overwhelm the cooling of the cables leading to a thermal runaway condition in which the cable quenches. In these measurements, voltage is measured over the terminations that includes part of the contact resistance of the terminations. Therefore, the dissipation of the VIC-Coil is less than the measured 70 mW m^{-1} at 65 K. Because the dropouts of I_c are sporadic in location and magnitude, a more detailed analysis is ongoing including determining the performance limitations due I_c dropouts not only from intrinsic dropouts, but also due to resistive joints between tapes [8, 24].

5. Conclusion

The results demonstrate the viability and effectiveness of CORC® wires fabricated from REBCO tapes with VIC that can be operated to high currents despite containing intrinsic defects. The I_c performance of a 10 m long VIC-Coil was evaluated and compared to a Baseline-Coil with similar performance measured at 76 K and 65 K. A VIC-Magnet was then tested and achieved stable performance at 4021 A (87% I_c) and successfully reached a peak magnetic field at I_c of 4.6 T at 25 K. Current-sharing between tapes facilitated by the cable's unique structure effectively manages localized I_c variations, ensuring magnet operation with low dissipation despite being operated above the sum tape I_c minima. The results substantiate that CORC® technology can effectively utilize REBCO tapes containing dropouts, significantly enhancing the economic feasibility and reliability of long-length HTS conductor production for applications such as fusion reactors, power transmission lines, and advanced rotating machinery.

Data availability statement

All data that support the findings of this study are included within the article (and any supplementary files).

Acknowledgment

This work was supported by the National High Magnetic Field Laboratory, which is supported by National Science Foundation through NSF/DMR-1644779 and by the US Department of Energy under Grant Numbers DE-EE0007872, DE-SC0019934, and DE-SC0014009.

Appendix

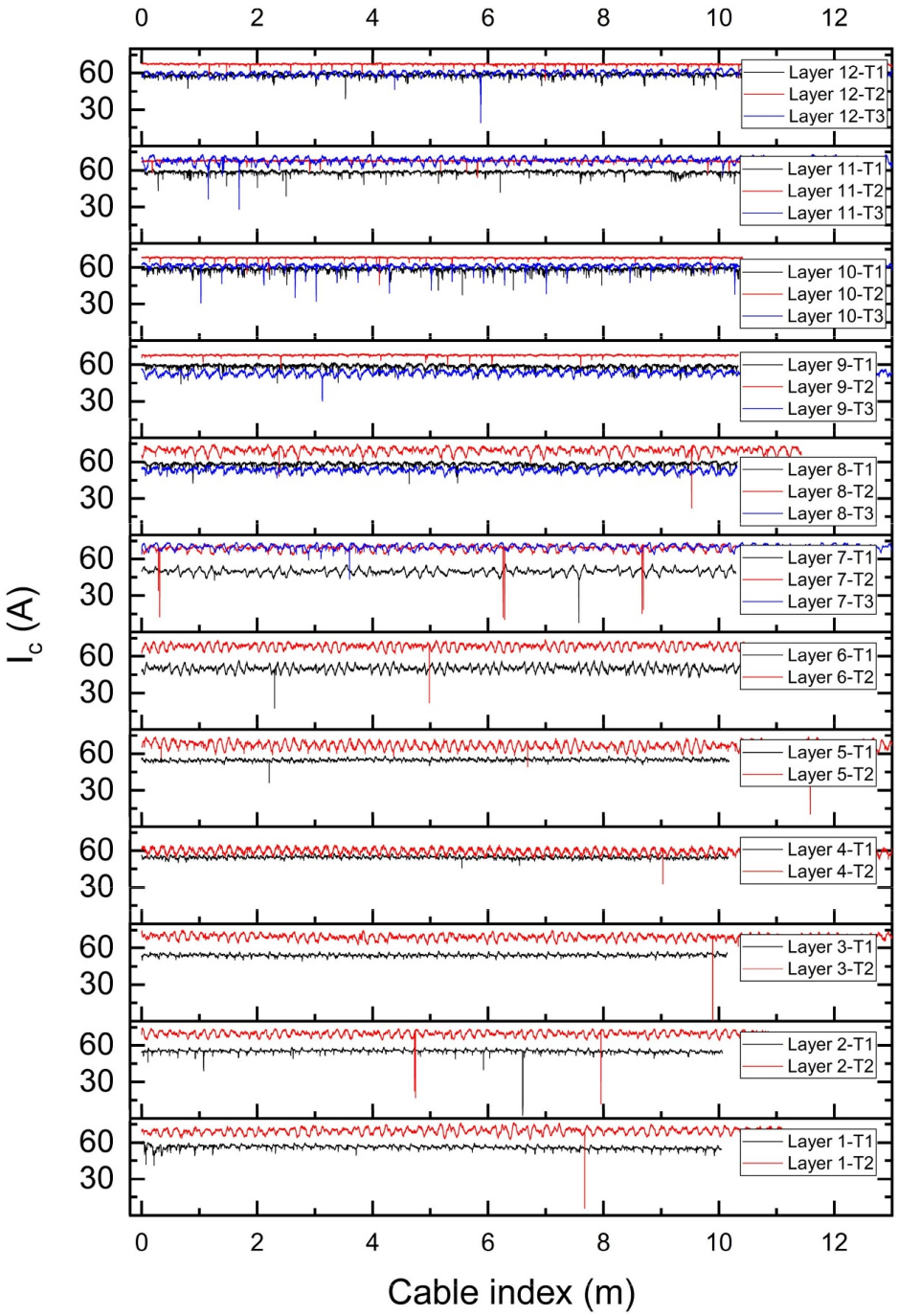

Figure A14. I_c as a function of CORC® wire index for all 30 tapes within the 10 m long VIC-Wire. Layers 1–6 contained two tapes each (T1, T2), while layers 7–12 contained three tapes each (T1, T2, T3).

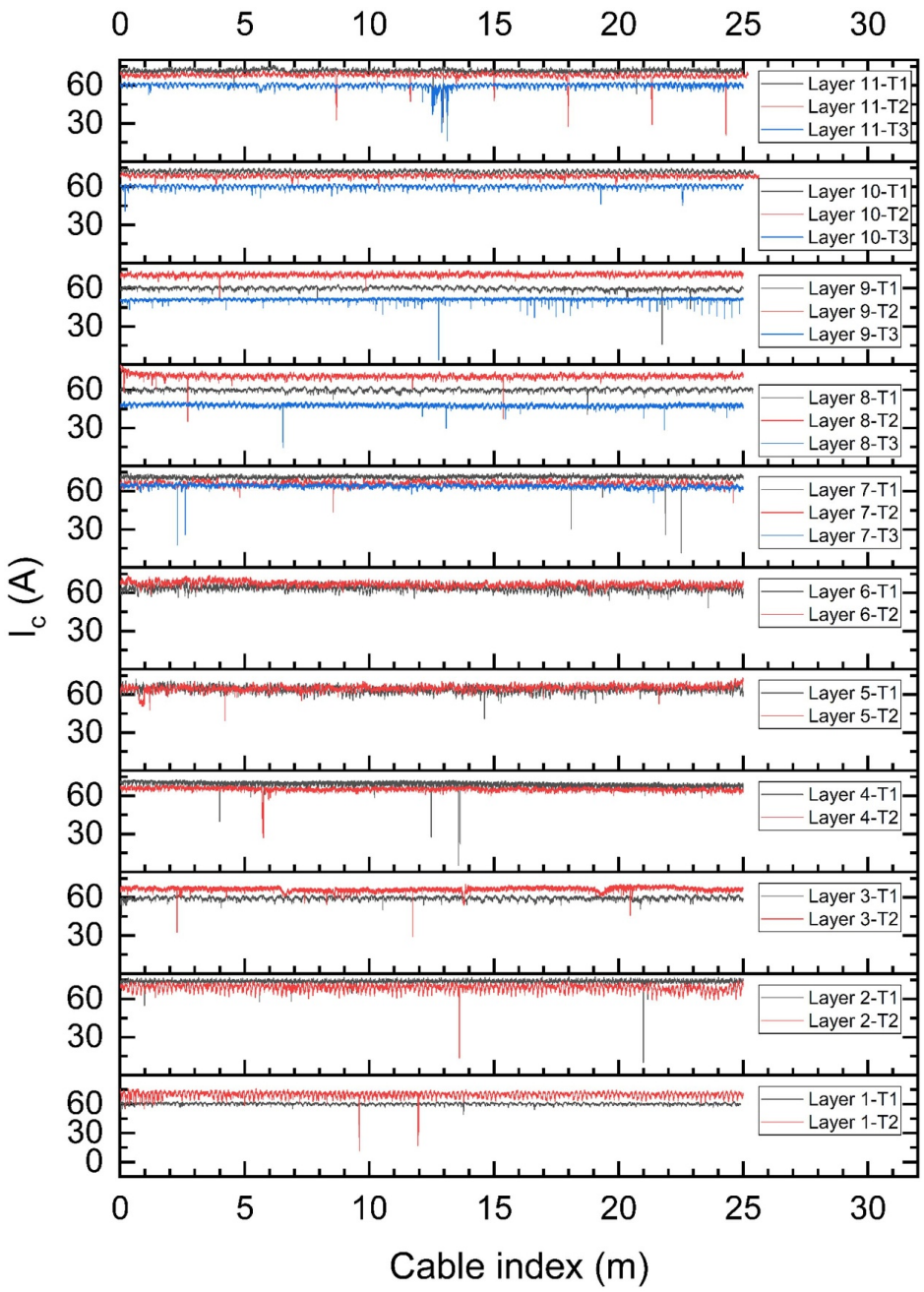

Figure A15. I_c as a function of CORC® wire index for all 27 tapes within the 25 m long VIC-Magnet. Layers 1–6 contained two tapes each (T1, T2), while layers 7–11 contained three tapes each (T1, T2, T3).

ORCID iDs

Jeremy D Weiss 0000-0003-0026-3049
Danko van der Laan 0000-0001-5889-3751
Chul H Kim 0000-0002-2122-5052
Reed Teyber 0000-0001-6924-4175
Virginia Phifer 0000-0002-9755-8072
Daniel S Davis 0000-0001-6152-8851
Yifei Zhang 0000-0001-9523-4878
Lance D Cooley 0000-0003-3488-2980
Sastry V Pamidi 0000-0002-5748-8938

References

[1] Bray J W 2015 High-temperature superconducting motors and generators for power grid applications *Superconductors in the Power Grid* (Elsevier) pp 325–44

[2] Bruzzone P, Fietz W H, Minervini J V, Novikov M, Yanagi N, Zhai Y and Zheng J 2018 High temperature superconductors for fusion magnets *Nucl. Fusion* **58** 103001
[3] Maeda H and Yanagisawa Y 2014 Recent developments in high-temperature superconducting magnet technology (Review) *IEEE Trans. Appl. Supercond.* **24** 1–12
[4] Hahn S, Radcliff K, Kim K, Kim S, Hu X, Kim K, Abraimov D V and Jaroszynski J 2016 Defect-irrelevant' behavior of a no-insulation pancake coil wound with REBCO tapes containing multiple defects *Supercond. Sci. Technol.* **29** 105017
[5] Lu J, Levitan J, McRae D and Walsh R 2018 Contact resistance between two REBCO tapes: the effects of cyclic loading and surface coating *Supercond. Sci. Technol.* **31** 085006
[6] Lu J, Goddard R, Han K and Hahn S 2017 Contact resistance between two REBCO tapes under load and load cycles *Supercond. Sci. Technol.* **30** 045005
[7] Wang Y, Chan W K and Schwartz J 2016 Self-protection mechanisms in no-insulation (RE)Ba 2 Cu 3 O x high temperature superconductor pancake coils *Supercond. Sci. Technol.* **29** 045007
[8] Teyber R, Marchevsky M, Martinez A C A, Prestemon S, Weiss J and van der Laan D 2022 Numerical investigation of current distributions around defects in high temperature superconducting CORC® cables *Supercond. Sci. Technol.* **35** 094008
[9] Martínez A C A, Ji Q, Prestemon S O, Wang X and Maury Cuna G H I 2020 An electric-circuit model on the inter-tape contact resistance and current sharing for REBCO cable and magnet applications *IEEE Trans. Appl. Supercond.* **30** 1–5
[10] Phifer V, Small M, Bradford G, Weiss J, van der Laan D and Cooley L 2022 Investigations in the tape-to-tape contact resistance and contact composition in superconducting CORC® wires *Supercond. Sci. Technol.* **35** 065003
[11] Yagotintsev K, Anvar V A, Gao P, Dhalle M J, Haugan T J, Van Der Laan D C, Weiss J D, Hossain M S A and Nijhuis A 2020 AC loss and contact resistance in REBCO CORC®, Roebel, and stacked tape cables *Supercond. Sci. Technol.* **33** 085009
[12] Van der Laan D C, Radcliff K, Anvar V A, Wang K, Nijhuis A and Weiss J D 2021 High-temperature superconducting CORC® wires with record-breaking axial tensile strain tolerance present a breakthrough for high-field magnets *Supercond. Sci. Technol.* **34** 10LT01
[13] van der Laan D, Weiss J, Radcliff K and Abraimov D 2024 CORC® wires allowing bending to 20 mm radius with 97.5% retention in critical current and having an engineering current density of 530 A mm−2 at 20 T *Supercond. Sci. Technol.* **37** 115007
[14] Wang K, Gao Y, Luo W, Zhou Y and Nijhuis A 2021 Nonlinear contact behavior of HTS tapes during pancake coiling and CORC cabling *Supercond. Sci. Technol.* **34** 075003
[15] Mulder T, Dudarev A, Mentink M, Dhallé M and Kate H T 2016 Development of joint terminals for a new six-around-one ReBCO-CORC® cable-in-conduit conductor rated 45 kA at 10 T/4 K *IEEE Trans. Appl. Supercond.* **26** 4801704
[16] van der Laan D C, Weiss J D, Scurti F and Schwartz J 2020 CORC® wires containing integrated optical fibers for temperature and strain monitoring and voltage wires for reliable quench detection *Supercond. Sci. Technol.* **33** 085010
[17] Willering G, van der Laan D C, Weijers H W, Noyes P D, Miller G E and Viouchkov Y 2015 Effect of variations in terminal contact resistances on the current distribution in high-temperature superconducting cables *Supercond. Sci. Technol.* **28** 035001
[18] Wimbush S C, Strickland N M and Pantoja A 2024 A high-temperature superconducting (HTS) wire critical current database *figshare* (https://doi.org/10.6084/m9.figshare.c.2861821.v19)
[19] van der Laan D C, Weiss J D and McRae D M 2019 Status of CORC® cables and wires for use in high-field magnets and power systems a decade after their introduction *Supercond. Sci. Technol.* **32** 033001
[20] Voran A, Weijers H W, Markiewicz W D, Gundlach S R, Jarvis J B and Sheppard W R 2017 Mechanical support of the NHMFL 32 T superconducting magnet *IEEE Trans. Appl. Supercond.* **27** 1–5
[21] Cheng J L 2022 HTS requirements for fusion magnets *Low Temperature Superconducting workshop*
[22] Molodyk A *et al* 2021 Development and large volume production of extremely high current density YBa2Cu3O7 superconducting wires for fusion *Sci. Rep.* **11** 2084
[23] van der Laan D C *et al* 2020 A CORC® cable insert solenoid: the first high-temperature superconducting insert magnet tested at currents exceeding 4 kA in 14 T background magnetic field *Supercond. Sci. Technol.* **33** 05LT03
[24] Weiss J 2024 Development and testing of high temperature superconducting CORC magnets and CICC for fusion applications *Applied Superconductivity Conf.* (available at: www.advancedconductor.com/wp-content/uploads/2024/11/Weiss-ASC-2024.pdf)